INFLAMED FAT: immune modulation of adipose tissue and lipid metabolism

Dam, A.D. van; Dam A.D. van

Chapter 2

BCG lowers plasma cholesterol levels and delays atherosclerotic lesion progression in mice

Andrea D. van Dam, Siroon Bekkering, Malou Crasborn, Lianne van Beek, Susan M. van den Berg, Frank Vrieling, Simone A. Joosten, Vanessa van Harmelen, Menno P.J. de Winther, Dieter Lütjohann, Esther Lutgens, Mariëtte R. Boon, Niels P. Riksen, Patrick C.N. Rensen, Jimmy F.P. Berbée

Atherosclerosis (2016) 251: 6-14

ABSTRACT

Bacille-Calmette-Guérin (BCG), prepared from attenuated live *Mycobacterium bovis*, modulates atherosclerosis development as currently explained by immunomodulatory mechanisms. However, whether BCG is pro- or anti-atherogenic remains inconclusive as the effect of BCG on cholesterol metabolism, the main driver of atherosclerosis development, has remained underexposed in previous studies. Therefore, we aimed to elucidate the effect of BCG on cholesterol metabolism in addition to inflammation and atherosclerosis development in *APOE*3-Leiden.CETP* mice, a well-established model of human-like lipoprotein metabolism. To this end, hyperlipidemic *APOE*3-Leiden.CETP* mice were fed a Western-type diet containing 0.1% cholesterol and were terminated 6 weeks after a single intravenous injection with BCG (0.75 mg; $5x10^6$ CFU). BCG-treated mice exhibited hepatic mycobacterial infection and hepatomegaly. The enlarged liver (+53%, p=0.001) coincided with severe immune cell infiltration and a higher cholesterol content (+31%, p=0.03). Moreover, BCG reduced plasma total cholesterol levels (-34%, p=0.003), which was confined to reduced nonHDL-cholesterol levels (-36%, p=0.002). This was due to accelerated plasma clearance of cholesterol from intravenously injected [^{14}C]cholesteryl oleate-labelled VLDL-like particles ($t_{½}$ -41%, p=0.002) as a result of elevated hepatic uptake (+25%, p=0.05) as well as reduced intestinal cholestanol and sterol absorption (up to -37%, p=0.003). Ultimately, BCG decreased foam cell formation of peritoneal macrophages (-18%, p=0.02) and delayed atherosclerotic lesion progression in the aortic root of the heart. BCG tended to decrease atherosclerotic lesion area (-59%, p=0.08) and reduced lesion severity. In conclusion, BCG reduces plasma nonHDL-cholesterol levels and delays atherosclerotic lesion formation in hyperlipidemic mice.

INTRODUCTION

Cardiovascular disease is the leading cause of death in Western countries, and atherosclerosis is the pathology underlying most cardiovascular events. The main risk factor for the development of atherosclerosis is hypercholesterolemia, as excess cholesterol initiates foam cell formation in the arterial wall. Subsequently, inflammatory processes including recruitment of innate and adaptive immune cells contribute to further development of the plaque, which may eventually lead to plaque rupture and/or vessel occlusion (1). A variety of bacteria and viruses (2), but also bacterial components such as lipopolysaccharide (3), have been suggested to be implicated in atherosclerosis development. In this respect, Bacille-Calmette-Guérin (BCG), prepared from attenuated live *Mycobacterium bovis* and the only licensed vaccine against tuberculosis (4), is of special interest since BCG is used worldwide for vaccination.

Interestingly, animal studies have shown that BCG modulates atherosclerosis development. However, the data on whether BCG reduces or enhances atherosclerosis development are conflicting. BCG injection in rabbits in which plasma cholesterol levels were maintained constant (*i.e.* by individual adjustment of the percentage of cholesterol in the diet) increased lymphocyte and monocyte activation and hence atherosclerosis development (5). In contrast, repeated injections of killed BCG reduced atherosclerosis in LDL receptor-knockout (*Ldlr*$^{-/-}$) and apolipoprotein E-knockout (*Apoe*$^{-/-}$) mice, but did not significantly modulate plasma cholesterol levels. The reduced atherosclerosis development was accompanied by enhanced circulating IL-10 levels and reduced serum levels of pro-inflammatory cytokines (6). Although these pro- and anti-atherogenic effects have been attributed to immunomodulatory effects of BCG, the effect of BCG on the metabolism of cholesterol, the main driver of atherosclerosis development, has remained underexposed.

Therefore, in the current study we aimed to elucidate the effect of BCG on cholesterol metabolism and atherosclerosis development in *APOE*3-Leiden.CETP* (*E3L.CETP*) transgenic mice. These mice have a humanized lipoprotein profile due to expression of human cholesterol ester transfer protein (CETP), which transfers cholesteryl esters from HDL to LDL and VLDL in exchange for triglycerides, and a mutation of the human *APOE*3* gene, which attenuates clearance of cholesterol-enriched lipoprotein remnants without abrogating the apoE-LDLR clearance pathway (7-9). We show that BCG markedly reduces plasma cholesterol levels as a result of accelerated hepatic uptake of cholesterol-enriched lipoprotein remnants and reduced intestinal cholesterol absorption. Finally, BCG reduces foam cell formation and delays atherosclerotic plaque formation.

MATERIALS AND METHODS

Mice, diet and BCG treatment

Female *E3L.CETP* mice were obtained as previously described (7, 8). At the start of the experiment mice were 10-12 weeks of age and housed under standard conditions with a 12:12 h light-dark cycle and free access to food and water. Mice were fed a Western-type diet containing 0.1% cholesterol (WTD; Hope Farms, The Netherlands). After a run-in period of 3 weeks with WTD, mice were randomized according to body weight, plasma total cholesterol (TC) and plasma triglycerides (TG), and received an intravenous injection with a human dose of Bacille-Calmette-Guérin (BCG) vaccine SSI (0.75 mg; $5x10^6$ CFU in 100 µL PBS; SSI Denmark) (10). Mice were terminated 6 weeks after the injection. Mouse experiments were performed in accordance with the Institute for Laboratory Animal Research Guide for the Care and Use of Laboratory Animals and had received approval from the University Ethical Review Board (Leiden University Medical Center, The Netherlands).

Mycobacterial culture

Blood, splenocytes and bone marrow were incubated both in BBL Bactec MGIT tubes (245113, BD and Company, NJ, USA) and on Lowenstein-Jensen + PACT plates (220501, BD and Company, NJ, USA) at 36°C. Bacterial growth in the BBL Bactec MGIT tubes was measured weekly using the BD BACTEC™-MicroMGIT Fluorescence Reader according to the manufacturer's instructions. Lowenstein-Jensen plates were checked once a week for growth of colonies. When positive, standard Ziehl-Neelsen (ZN) staining [z1] was performed to confirm presence of mycobacteria.

Liver histology

Livers were fixed in 4% paraformaldehyde, dehydrated in 70% EtOH, and embedded in paraffin. Hematoxylin-eosin (HE) and ZN stainings were performed on sections (5 µm) using standard protocols. Immunohistochemical detection of F4/80 was done on paraffin-embedded sections that were treated with proteinase K, by using a primary rat anti-

Table 1: *Primer sequences of forward and reverse primers (5' → 3').*

Gene	Forward primer	Reverse primer
Apob	GCCCATTGTGGACAAGTTGATC	CCAGGACTTGGAGGTCTTGGA
Cd3	AACACGTACTTGTACCTGAAAGCTC	GATGATTATGGCTACTGCTGTCA
Cd4	ACACACCTGTGCAAGAAGCA	GCTCTTGTTGGTTGGGAATC
Cd8	GGCTCTGGCTGGTCTTCA	GACGAAGGGGTCTGAATGAG
F4/80	CTTTGGCTATGGGCTTCCAGTC	GCAAGGAGGACAGAGTTTATCGTG
Gapdh	GGGGCTGGCATTGCTCTCAA	TTGCTCAGTGTCCTTGCTGGGG
Hmgcoar	CCGGCAACAACAAGATCTGTG	ATGTACAGGATGGCGATGCA
Ldlr	GCATCAGCTTGGACAAGGTGT	GGGAACAGCCACCATTGTTG
Tnf	AGCCCACGTCGTAGCAAACCAC	TCGGGGCAGCCTTGTCCCTT

mouse F4/80 monoclonal Ab (MCA497; 1/600, Serotec, UK) and a secondary goat anti-rat immunoglobulin peroxidase (MP-7444, Vector Laboratories Inc., CA, USA). The peroxidase activity was revealed with NovaRed (SK-4800, Vector Laboratories Inc.) and slides were counterstained with hematoxylin. The area positive for F4/80 was quantified using ImageJ Software.

RNA purification and quantitative RT-PCR

RNA was extracted from snap-frozen mouse livers using Tripure RNA Isolation reagent (Roche, The Netherlands) according to manufacturer's instructions. RNA concentrations were measured using NanoDrop and RNA was reverse transcribed using Moloney Murine Leukemia Virus Reverse Transcriptase (Promega, The Netherlands) for quantitative RT-PCR (qRT-PCR) to produce cDNA. Expression levels of genes were determined by qRT-PCR, using gene-specific primers (**Table 1**) and SYBR green supermix (Biorad, The Netherlands). mRNA expression was normalized to *Gapdh* mRNA content and expressed as fold change compared with control mice using the $\Delta\Delta$CT method.

Flow cytometry

Circulating white blood cells were analysed using flow cytometry. After lysis of red blood cells, pelleted cells were resuspended in FACS buffer and stained for 30 minutes at 4°C in the dark with the fluorescently labelled antibodies listed in **Table 2**. Cells were measured on an LSR II flow cytometer (BD Biosciences, CA, USA). Data were analysed using FlowJo software (Treestar, OR, USA).

Isolation and ex vivo stimulation of cells

Resident peritoneal macrophages were isolated from mice by washing the peritoneal cavity with ice-cold sterile PBS. Pelleted cells were resuspended in RPMI 1640 Dutch-modified culture medium (Life Technologies/Invitrogen, The Netherlands) supplemented with 10

Table 2: *Antibodies used for flow cytometry.*

Antibody	Fluorochrome	Dilution	Clone, supplier
CD45.2	FITC	1:100	104, BioLegend
CD3	APC	1:100	145-2C11, eBioscience
CD4	Qdot605	1:1000	RM-4-5, BioLegend
CD8a	PerCPCy5.5	1:100	53-6.7, BioLegend
CD25	PeCy7	1:300	PC61.5, eBioScience
CD44	eFluor450	1:300	IM7, eBioScience
CD22.2	PE	1:200	Cy34.1, BD Biosciences
Cd11b	Pacific Blue	1:150	M1/70, BioLegend
Cd115-Biotin	n.a.	1:100	AFS98, eBioScience
Streptavidin	PeCy5	1:100	SAV, eBioScience
Gr-1	PeCy7	1:1500	RB6-8C5, Biolegend

mM glutamine, 10 mM pyruvate (Invitrogen) and 10 µg/mL gentamicin (Centrafarm, The Netherlands) and stimulated with 10 ng/mL LPS (*E. coli* serotype 055:B5, further purified as described previously (11); Sigma-Aldrich, MO, USA) for 24 h. Supernatants were collected for determination of cytokine secretion.

Splenocytes were resuspended in RPMI and stimulated with 10 ng/mL LPS or heat-inactivated *C. albicans* (MYA-3573 UC 820, ATCC, Germany). Supernatants were collected at 48 h or 5 days for measurement of innate or adaptive cytokines.

Bone marrow cells were resuspended in Dulbecco's Modified Eagle Medium (Gibco, Invitrogen, CA, USA) supplemented with 30% L929 medium, 10% FCS, 1% nonessential amino acids, 1% 100 U/mL penicillin and 100 mg/mL streptomycin for differentiation into macrophages. On day 6, the bone marrow-derived macrophages (BMDMs) were harvested and stimulated with 10 ng/mL LPS for 24 h. Supernatants were collected for cytokine measurements.

Cytokine measurements

Mouse IL-6 (CMC0063, Life technologies, The Netherlands), IL-10 and interferon γ (IFNγ; DY417 and DY485, R&D Systems Europe, UK) were measured using commercial ELISA kits according to manufacturers' instructions. Mouse tumor necrosis factor alpha (TNF) and IL-1β were measured using specific radioimmunoassays (RIA) as described previously (12).

Food intake and body weight and composition measurements

Food intake and body weight were measured weekly with a scale, and body composition was measured using an EchoMRI-100 analyzer (EchoMRI, TX, USA).

Determination of plasma and liver lipids

At the indicated time points, 4 h-fasted (from 8:00 am to 12:00 pm) blood samples were collected through tail vein bleeding and isolated plasma was assayed for TC and TG by using commercially available enzymatic kits (Roche Diagnostics, Germany). For determination of HDL-cholesterol, apoB-containing particles were precipitated from plasma with 20% polyethylene glycol in 200 mM glycine buffer (pH 10) and TC was measured in the supernatant.

Lipids were extracted from the liver following a protocol modified from Bligh and Dyer (13). Liver samples were homogenized in 10 µL ice-cold CH_3OH/mg tissue. Lipids were extracted into an organic phase by the addition of 1,800 µL CH_3OH:$CHCl_3$ (1:3 v/v) to 45 µL homogenate and subsequent centrifugation. The lower organic phase was evaporated, lipids were resuspended in 2% Triton X-100, and TC and TG content was assayed as described above. Phospholipids (PL) were determined using an enzymatic colorimetric kit (Instruchemie, The Netherlands).

Table 3: *Primary antibodies used for Western blot.*

Primary antibody	Dilution	Supplier
LDLR	1:1000	AF2255, R&D Systems
SR-BI	1:1000	Ab396, Abcam Inc
α/β-Tubulin	1:1000	#2148, Cell Signaling

In vivo clearance of VLDL-like particles

VLDL-like TG-rich particles (80 nm) labelled with glycerol tri[^{3}H]oleate (TO) and [^{14}C] cholesteryl oleate (CO) were prepared and characterized as described previously (9, 14). Mice were fasted for 4 h (from 8:00 am to 12:00 pm) and injected with 200 µL of VLDL-like particles (1.0 mg TG per mouse) via the tail vein. Blood samples were drawn from the tail vein at the indicated times after injection to determine the plasma decay of [^{3}H]TO and [^{14}C]CO. After 15 min, mice were killed by cervical dislocation and perfused with ice-cold PBS through the heart. Organs were harvested and weighed, dissolved in Tissue Solubilizer (Amersham Biosciences, The Netherlands) overnight at 56°C and analysed for ^{3}H- and ^{14}C-activity.

Extraction and analysis of hepatic cholestanol and sterols

Total cholesterol, markers for hepatic cholesterol synthesis (*i.e.* lanosterol, desmosterol and lathosterol) as well as markers for intestinal cholesterol absorption (*i.e.* cholestanol, campesterol and sitosterol) were extracted from liver by chloroform-methanol and analysed by GC-flame ionization detection and GC-MS as reported previously (15). Dry weight of liver samples was determined after they were dried to constant weight overnight in a Speedvac (Servant Instruments Inc., NY, USA). Data are expressed as ratio to hepatic total cholesterol levels.

Western blot

Pieces of snap-frozen liver tissue (~50 mg) were lysed, protein was isolated, and Western blots were performed as previously described (16). Primary antibodies and dilutions are listed in **Table 3**. Protein content was corrected for the housekeeping protein Tubulin.

Assessment of foam cell formation

Foam cell formation was assessed by culturing 1x10^{5} cells/well either in control medium or medium supplemented with 50 µg/mL oxidized human LDL (oxLDL, prepared as described previously (17)) for 48 h. Supernatants were removed and cells were lysed (0.5% Triton-X100). Uptake of oxidized LDL was assessed by measuring intracellular human apoB with ELISA as described before (17).

Atherosclerosis quantification

Hearts were collected, fixed in 4% paraformaldehyde, dehydrated in 70% EtOH, embedded in paraffin and cross-sectioned (5 µm) perpendicular to the axis of the aorta throughout the aortic root area, starting at the point where the open aortic valve leaflets appear. Per mouse, four sections with 50 µm intervals were used for atherosclerosis measurements. Sections were stained with haematoxylin-phloxine-saffron (HPS) for histological analysis. Lesions were categorized for lesion severity according to the guidelines of the American Heart Association adapted for mice (18). Various types of lesions were discerned: mild lesions (types 1-3), severe lesions (types 4-5) and valve lesions. Lesion area was determined using ImageJ Software (9). Detection of macrophage-positive area was performed with rat monoclonal anti-MAC-3 antibody (BD Pharmingen, CA, USA) and Vector Impress anti-rat (Vector Laboratories Inc.). The immunostaining was amplified using Vector Laboratories Elite ABC kit and peroxidase activity was visualized with NovaRed (Vector Laboratories Inc.). Sirius red (Chroma, Germany) was used to stain for collagen. The stability index was determined by dividing the Sirius red-positive area by the MAC-3-positive area.

Statistical Analysis

All data are expressed as means ± SEM. Groups were compared with a two-tailed unpaired Student's t-test unless stated otherwise. Groups were considered statistically significant if $p<0.05$.

RESULTS

BCG induces mycobacterial infection in hyperlipidemic mice

E3L.CETP mice were fed a Western-type diet containing 0.1% cholesterol (WTD) and received a single intravenous BCG injection. After six weeks, blood and various organs were cultured to investigate whether viable BCG was still present. Blood of BCG-treated mice tested negative for mycobacteria. However, livers, spleens and bone marrow of BCG-treated mice were positive for mycobacteria (**Suppl. Fig. 1** and data not shown), indicating ongoing infection.

BCG induces hepatic inflammation

Since BCG induced hepatic mycobacterial infection and the liver plays a key role in lipid metabolism, we further studied the livers of the BCG-treated animals. Liver weight was increased in BCG-treated mice (+53%, **Fig. 1A**). In these livers, severe leukocyte infiltration (**Fig. 1B**) and accumulation of F4/80-positive cells (**Fig. 1C**) was observed. This coincided with increased expression of inflammatory markers including *F4/80* and *Tnf* as well as the T cell markers *Cd3*, *Cd4* and *Cd8* (**Fig. 1D**). Besides hepatomegaly, BCG-treated mice also exhibited an enlarged spleen (+149%, **Fig. 1A**).

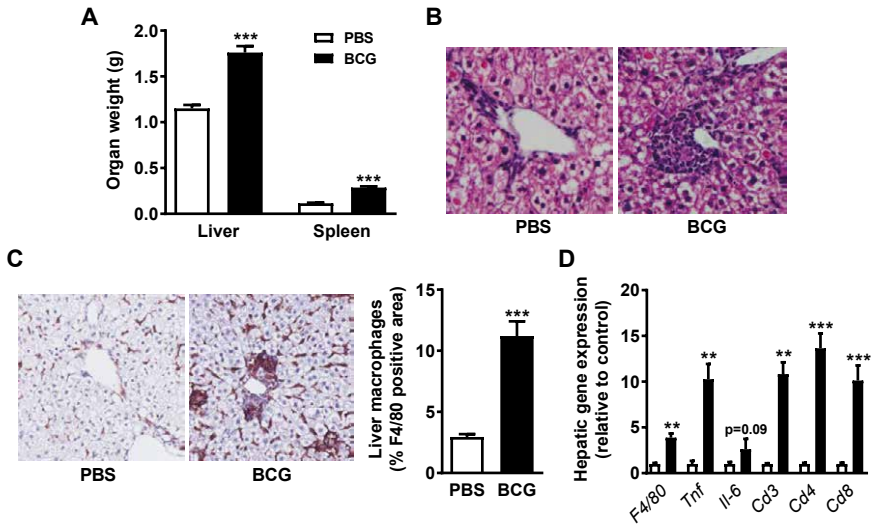

Figure 1. BCG induces hepatic inflammation. *E3L.CETP mice fed a WTD were treated with PBS or BCG (0.75 mg; 5x10⁶ CFU; i.v.). Upon sacrifice after 6 weeks, liver and spleen were collected and weighed (A). Haematoxylin and Eosin (B) and F4/80 staining (C) of liver sections was performed. Representative pictures are shown. The relative content of F4/80 positive cells was quantified (C). Hepatic mRNA expression of the indicated inflammatory genes was determined (D). Values represent means ± SEM (n=6). **p<0.01 ***p<0.001 vs. PBS.*

BCG induces overall immune activation

Given the inflammatory state of the liver, we assessed the effect of BCG on circulating white blood cells by flow cytometry. Within the CD45⁺ white blood cells, BCG did not significantly affect the relative monocyte or granulocyte content (**Suppl. Fig. 2A, B**), but did reduce the percentage of B cells (-33%, **Suppl. Fig. 2C**). The percentage of total T cells remained similar upon BCG vaccination (**Suppl. Fig. 2D**), but BCG increased T helper cells (+11%, **Fig. 2A**) without altering cytotoxic T cells (**Fig. 2D**). Activation of T helper cells was not affected by BCG (**Fig. 2B**), but the memory T helper cells tended to be higher (+59%, **Fig. 2C**). More pronounced effects on activation and memory were found within the cytotoxic T cells, as BCG induced both activation (+204%, **Fig. 2E**) and memory (+84%, **Fig. 2F**) of cytotoxic T cells. Overall, these findings suggest that BCG induces activation of circulating immune cells.

To determine the inflammatory status of tissue macrophages, we performed *ex vivo* stimulation of peritoneal macrophages, splenocytes and bone marrow-derived macrophages and measured cytokine secretion. BCG increased the number of macrophages in the peritoneal cavity (+37%, **Fig. 2G**). Even after correcting for the number of cells, the peritoneal macrophages of BCG-treated mice produced more inflammatory cytokines upon LPS stimulation than macrophages from untreated animals (*i.e.* TNF, IL-1β; **Fig. 2H-K**), suggesting an increased innate inflammatory phenotype.

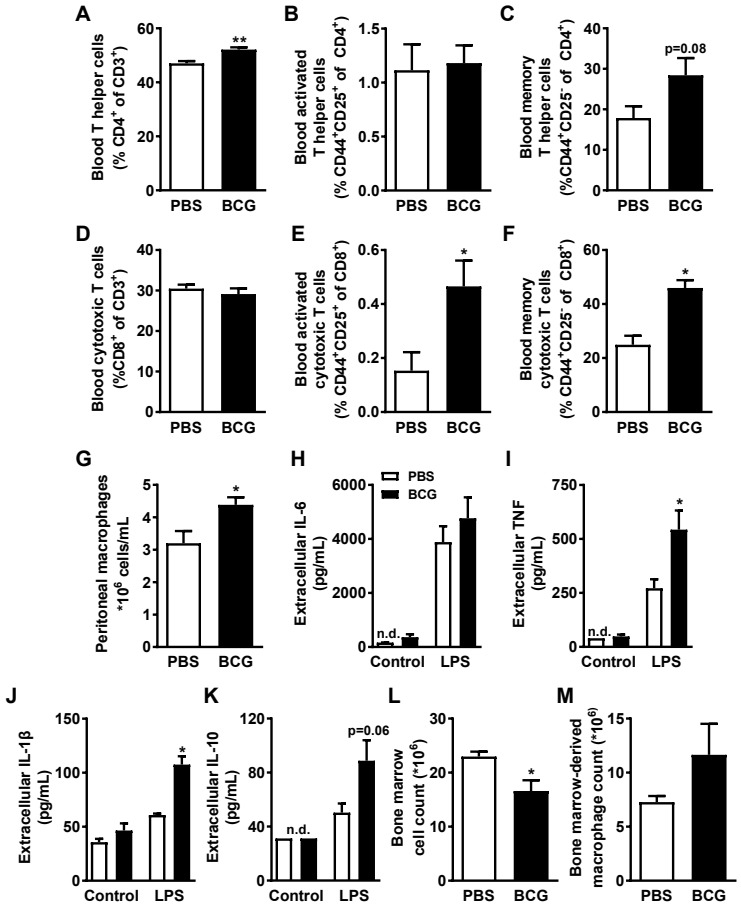

Figure 2. BCG increases immune activation. *E3L.CETP mice fed a WTD were treated with PBS or BCG (0.75 mg; 5x10⁶ CFU; i.v.). After 6 weeks, blood, peritoneal macrophages and bone marrow were collected. Within the CD3⁺ T cell fraction, percentage of CD4⁺ (A) and CD8⁺ (D) cells were determined. Within the CD4⁺ and CD8⁺ T cell fractions, percentages of activated T cells (CD44⁺CD25⁺; B, E) and memory T cells (CD44⁺CD25⁻; C, F) were determined. Peritoneal macrophages were counted (G) and stimulated with LPS. Production of IL-6 (H), TNF (I), IL-1β (J) and IL-10 (K) was measured. Bone marrow cells were counted before (L) and after differentiation into macrophages (M). Values represent means ± SEM (n=6). *p<0.05 **p<0.01 vs. PBS.*

Splenocytes from BCG-treated mice also produced more inflammatory cytokines upon LPS stimulation (*i.e.* IL-6, TNF, IL-10; **Suppl. Fig. 2E-G**), confirming the inflammatory phenotype. Interestingly, upon adaptive immune response stimulation (*i.e.* with *C. Albicans*) splenocytes also produced more IFNγ (**Suppl. Fig. 2H**), suggesting that BCG activates $CD4^+$ and $CD8^+$ T cells in the spleen, in line with our observations on circulating cells.

Bone marrow cell counts were lower in mice treated with BCG (-28%, **Fig. 2L**). After adjusting for the number of cells, bone marrow-derived macrophages (BMDMs) from BCG treated mice did not exhibit lower capacity to proliferate (**Fig. 2M**), suggesting that the reduced bone marrow cell counts reflect hematopoietic stem and progenitor cell exhaustion. LPS stimulation of BMDMs did not reveal alterations in cytokine production (data not shown). Taken together, BCG infection resulted in increased overall immune activation.

BCG lowers body fat but increases liver lipid content

To assess the effect of BCG on the metabolic phenotype of *E3L.CETP* mice, body weight and composition were measured over the 6-week period after BCG administration. Total body weight (**Fig. 3A**) and food intake (**Fig. 3B**) were not affected by BCG. After 6 weeks, lean body mass remained unaffected (**Fig. 3C**), but fat mass tended to be lower in BCG-treated animals (-32%, **Fig. 3D**), which was corroborated by a reduced weight of the gonadal white

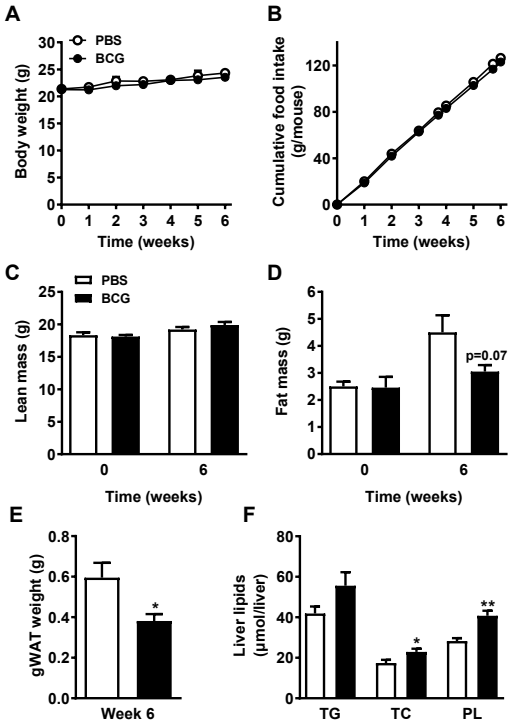

Figure 3. BCG increases liver lipids. *E3L.CETP mice fed a WTD were treated with PBS or BCG (0.75 mg; 5x10⁶ CFU; i.v.). Body weight (A), food intake (B), lean mass (C), fat mass (D), gonadal white adipose tissue weight (E) were measured at the indicated time points. Lipids were extracted from liver and liver triglycerides (TG), liver total cholesterol (TC) and liver phospholipids (PL) were measured (F). Values represent means ± SEM (n=5-6). *p<0.05 **p<0.01 vs. PBS. gWAT, gonadal white adipose tissue.*

fat pads (-36%, **Fig. 3E**). In line with the increase in liver weight, BCG-treated mice exhibited increased liver lipid content (*i.e.* TG, cholesterol and phospholipids), although the increase in TG content did not reach statistical significance (**Fig. 3F**).

BCG lowers plasma cholesterol by accelerating hepatic uptake of cholesterol-enriched lipoprotein remnants and reducing intestinal cholesterol absorption

As hypercholesterolemia is the main risk factor for atherosclerosis development, we studied the effect of BCG on plasma lipid levels. BCG tended to decrease plasma TG levels after 6 weeks (-34%, **Fig. 4A**), and consistently reduced plasma total cholesterol (TC) levels during the study (-34% at the endpoint, **Fig. 4B**) when compared to the PBS-treated group. This reduction in TC was confined to lowering of the nonHDL-cholesterol fraction (**Fig. 4C**). To investigate whether the reduced plasma TC levels were due to increased clearance of lipoprotein remnant cholesterol, we assessed the plasma clearance and organ uptake of glycerol tri[^{3}H]oleate (TO)- and [^{14}C]cholesteryl oleate (CO)-double-labelled VLDL-like particles *in vivo*. Plasma clearance of [^{3}H]TO was comparable between the groups (**Fig. 4D**, $t_{½}$ = 3.0 *vs.* 3.4 min, p=0.09), and no obvious effects on organ uptake of ^{3}H-activity were found apart from an increased uptake by the spleen (+109%, **Fig. 4E**). In contrast, BCG markedly accelerated plasma clearance of [^{14}C]CO (**Fig. 4F**, $t_{½}$ = 5.0 *vs.* 8.5 min, p=0.002), mainly due to increased uptake of [^{14}C]CO by the liver (+25%, p=0.05) and to a lesser extent also by the spleen (+214%, **Fig. 4G**). The increase in liver and spleen weight are key to this increased [^{14}C]CO-uptake, as uptake of [^{14}C]CO by liver and spleen did not differ when expressed per gram organ (data not shown). These data support the notion that BCG reduces plasma TC levels by enhancing hepatic uptake of cholesterol-enriched lipoprotein remnants.

Besides increased cholesterol clearance, reduced hepatic cholesterol synthesis or intestinal cholesterol absorption could underlie the reduced plasma cholesterol levels. To assess whether BCG affects hepatic cholesterol synthesis, we determined the cholesterol precursors lanosterol, desmosterol and lathosterol in the liver (**Fig. 4H**). The ratios of lanosterol and desmosterol to total cholesterol were increased (+53 and +79%) upon BCG treatment, whereas the ratio of lathosterol to cholesterol remained unchanged. This suggests increased rather than decreased hepatic cholesterol synthesis. As measures of intestinal cholesterol absorption, we measured cholestanol, campesterol and sitosterol in the liver (**Fig. 4I**). Interestingly, the ratios of cholestanol and campestanol to total cholesterol were decreased (-28% and -37%), whereas the ratio of sitosterol to total cholesterol remained similar. These data indicate that BCG reduces intestinal cholesterol absorption.

We next assessed gene expression and protein content in the liver upon BCG treatment. BCG did not affect genes involved in cholesterol metabolism, including *Ldlr*, *Apob* and *Hmgcoar*, nor LDLR and SR-BI protein content (data not shown).

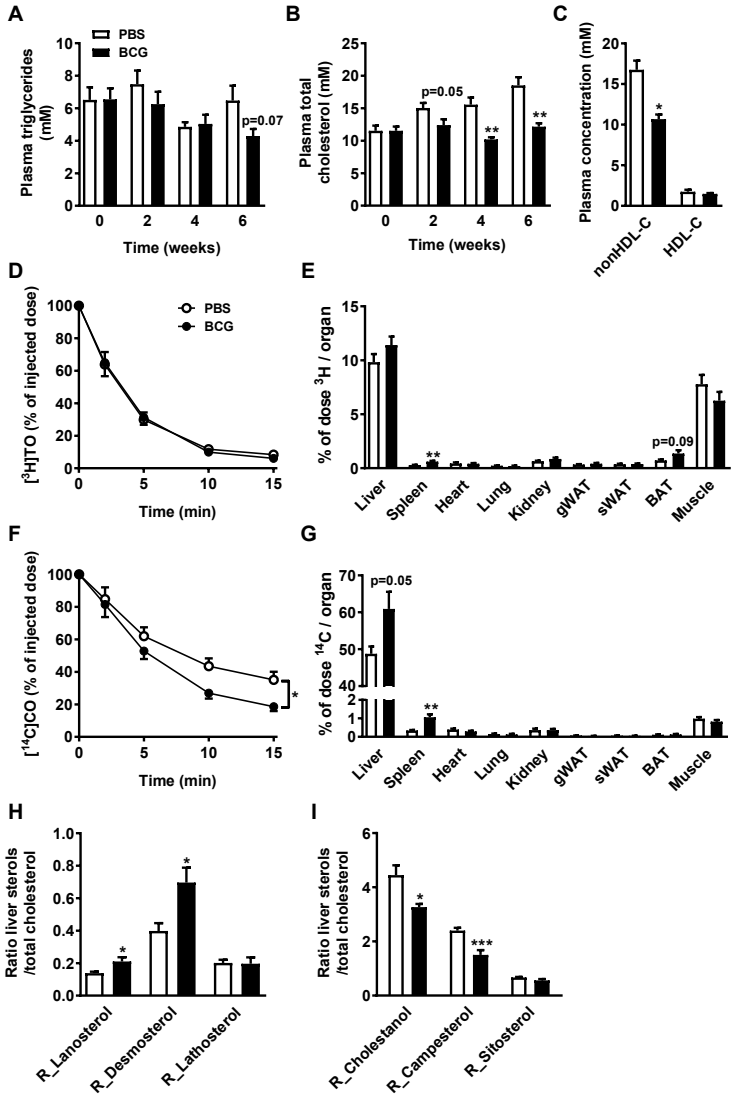

Figure 4. BCG increases plasma cholesterol clearance towards the liver and reduces intestinal cholesterol absorption. *E3L.CETP mice fed a WTD were treated with PBS or BCG (0.75 mg; 5x10⁶ CFU; i.v.). Plasma triglycerides (A) and total cholesterol (B) were analysed at the indicated time points. After 6 weeks of treatment also plasma nonHDL-cholesterol and HDL-cholesterol were determined (C). After 6 weeks, mice were injected with glycerol tri[³H]oleate and [¹⁴C]cholesteryl oleate double-labelled VLDL-like particles and clearance from plasma (D, F) and uptake by organs and tissues at 15 min after injection were determined by analysing ³H- and ¹⁴C-activity (E, G). Cholestanol and sterols were extracted from liver and expressed as ratios to cholesterol or per mg dry tissue weight (H, I). Values represent means ± SEM (n=4-6). Interaction between plasma clearance of ³H- and ¹⁴C-activity and time was analysed by two-way ANOVA. *p<0.05 **p<0.01 vs. PBS. nonHDL-C, nonHDL-cholesterol; HDL-C, HDL-cholesterol; gWAT, gonadal white adipose tissue; sWAT, subcutaneous white adipose tissue; BAT, brown adipose tissue.*

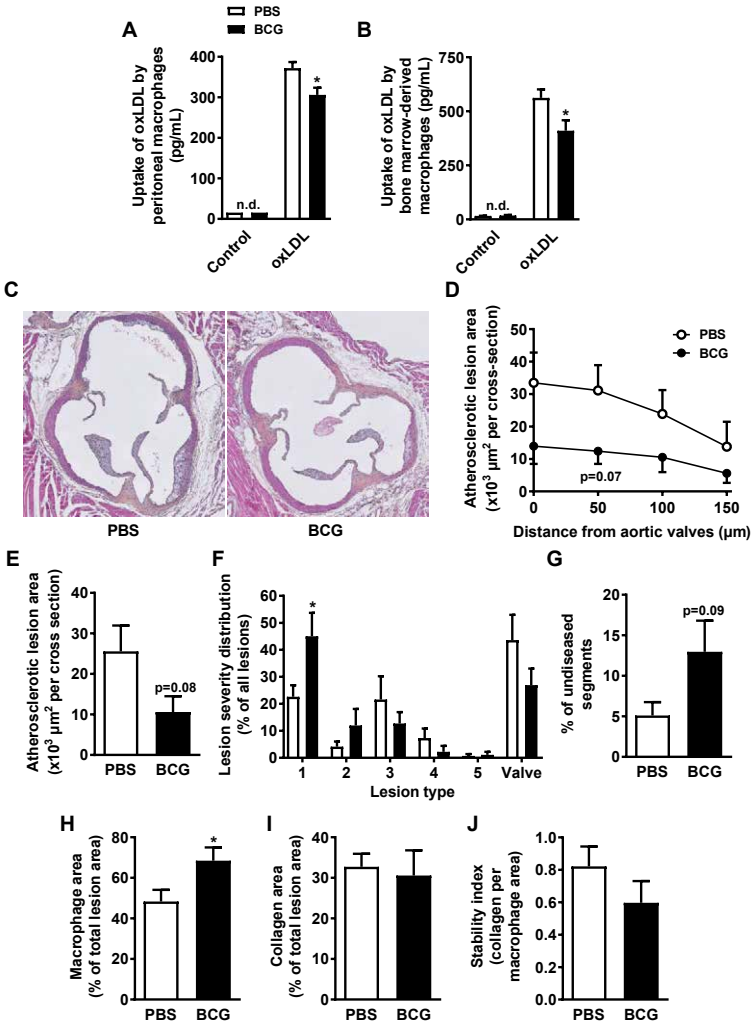

Figure 5. BCG decreases atherosclerosis development. *E3L.CETP mice fed a WTD were treated with PBS or BCG (0.75 mg; 5x10^6 CFU; i.v.). After 6 weeks, peritoneal macrophages (A) and bone marrow-derived macrophages (B) were incubated with oxLDL and uptake was measured. Hearts were collected and slides of the valve area of the aortic root of were stained with haematoxylin – phloxine – saffron (C). Atherosclerotic lesion area as a function of distance was determined (D) and the mean lesion area was calculated from the four cross-sections from D (E). Lesions were categorized according to lesion severity (F) and the percentage of non-diseased segments was scored (G). The macrophage (H) and collagen (I) content of the lesions was determined, and the stability index (collagen/macrophage content of the lesions) was calculated (J). Values represent means ± SEM (n=6). *p<0.05 vs. PBS.*

BCG delays atherosclerosis development

Since BCG markedly increased immune activation, but lowered plasma cholesterol levels, we investigated the effects of BCG on foam cell formation and atherosclerosis development. BCG reduced the *ex vivo* uptake of oxLDL by peritoneal macrophages (-18%, **Fig. 5A**) and BMDMs (-27%, **Fig. 5B**), suggesting reduced foam cell formation and an overall anti-atherogenic phenotype of macrophages after BCG treatment.

We therefore determined atherosclerotic lesion area of the lesions in the aortic root of the heart 6 weeks after BCG administration. Interestingly, BCG tended to reduce atherosclerotic lesion area throughout the aortic root (**Fig. 5C, D**) as well as the mean atherosclerotic lesion area (-59%, **Fig. 5E**). Although lesion severity was generally mild, BCG still induced a shift towards a reduced lesion severity (**Fig. 5F**). In addition, the number of non-diseased segments tended to be higher after BCG treatment (+155%, **Fig. 5G**). In line with the reduced lesion severity, BCG increased the macrophage content of the lesions (+43%, **Fig. 5H**). Collagen content (**Fig. 5I**) and lesion stability (ratio collagen/macrophage area, **Fig. 5J**) were not affected by BCG. When only type 3 lesions were compared between groups, the macrophage content and lesion stability were unaffected (data not shown), indicating that BCG did not induce a more inflammatory or unstable phenotype of the lesions. Together, our findings indicate that BCG administration decreases plasma cholesterol levels and delays atherosclerosis development.

DISCUSSION

BCG has been shown to modulate atherosclerosis development through immunomodulatory mechanisms (5, 6), but its effect on cholesterol metabolism, the main determinant of atherosclerosis, has not been investigated before. In the current study, we show that BCG administration in hyperlipidemic *E3L.CETP* mice induced an overall inflammatory phenotype, as shown by hepatic infection and inflammation, and activation of circulating T cells as well as peritoneal macrophages and splenocytes. Furthermore, BCG markedly decreased plasma nonHDL-cholesterol levels by enhancing hepatic clearance of cholesterol and reduced foam cell formation *ex vivo*. As a result of these anti-atherogenic characteristics, BCG delayed atherosclerosis progression and reduced lesion severity.

We found BCG to be present in the liver, spleen and bone marrow 6 weeks after administration, indicating that the mycobacterium disseminated to these organs. In humans, dissemination of BCG can occur upon vaccination (19-21) and disseminated BCG infections can manifest in bladder cancer patients as a side effect of intravesical treatment with BCG (22). Our finding that the liver and spleen were enlarged in the BCG-treated group has also been observed in humans upon disseminated BCG infection (21, 23) and extrapulmonary tuberculosis (24, 25). Together, these reports indicate that our study can be translated to the human situation.

Besides increased immune activation, we observed a large reduction of plasma nonHDL-cholesterol levels upon BCG administration, which was accompanied by elevated hepatic

uptake of circulating cholesterol-enriched lipoprotein remnants and reduced intestinal cholesterol absorption. Since plasma HDL-cholesterol nor hepatic SR-BI content were altered, it seems unlikely that BCG influences reverse cholesterol transport. An underlying mechanism for the reduced plasma nonHDL-cholesterol levels could be that accumulated immune cells (26) as well as mycobacteria (27-30), both of which we detected in the liver, are responsible for the increased hepatic lipoprotein remnant uptake. Immune cells use lipids as an energy source and cholesterol is indispensable as a membrane component for cell growth, proliferation and membrane remodelling (26, 31, 32). Mycobacteria use host cholesterol for entry into macrophages and as a source of carbon and energy, as they cannot synthesize cholesterol themselves (27, 28, 33). Therefore, host cholesterol is essential for the persistence of infection (27-29). For *mycobacterium leprae*, which also infects macrophages and uses host cholesterol for survival, it was recently shown that infected macrophages take up LDL by upregulation of LDLR (34). Furthermore, *Ldlr* expression was shown to be upregulated in caseous human pulmonary tuberculosis granulomas (35), supporting the possibility that upregulation of LDLR specifically in infected tissue macrophages underlies the increased cholesterol uptake in our study. An additional cause of the reduced plasma nonHDL-cholesterol levels is the reduced intestinal cholesterol absorption as evidenced by reduced cholestanol and plant sterol levels in the liver. Intestinal absorption can be dysregulated by systemic or intra-abdominal inflammation, which is also observed in coeliac disease, Crohn's disease (36) and cystic fibrosis patients (37, 38). Evidently, BCG infection and subsequent inflammation also lead to reduced cholesterol absorption.

Several pieces of evidence suggest that mycobacteria modulate lipid metabolism in humans as well. For instance, cholesterol levels in Nigerian adults with tuberculosis are lower when compared to healthy controls (39). Deniz *et al.* (40) also show that serum total cholesterol, HDL-cholesterol and LDL-cholesterol concentrations are lower in patients with pulmonary tuberculosis. Moreover, *M. tuberculosis* uses fatty acids from host triglycerides as a lipid source (41) and tuberculosis patients exhibit lower serum medium-chain fatty acids (42). Unfortunately, to our knowledge, no data exist on plasma cholesterol levels in patients with disseminated BCG infection.

Ultimately, BCG tended to reduce atherosclerotic lesion area by more than half, and delayed the onset and progression of atherosclerosis evidenced by 1) the increased number of non-diseased segments; 2) the higher percentage of mild type 1 lesions; 3) the increased macrophage content of the lesions, indicative for mild type 1 and 2 lesions. Although the latter could also point to a more inflammatory phenotype of the lesions, this was contradicted by the fact that the macrophage content and lesion stability index within type 3 lesions only did not differ between the groups. Previous studies that investigated the effect of BCG on atherosclerosis focussed on the immunomodulatory effects of BCG and were not properly designed to investigate the effect of BCG on cholesterol metabolism. In one study performed in rabbits, plasma cholesterol level of each individual rabbit was maintained at a specific level by adjusting the cholesterol content in the diet (5), excluding the possibility to investigate the effects of BCG on cholesterol metabolism. Ovchinnikova *et*

al. (6) studied the effect of BCG that was killed by extensive freeze-drying on atherosclerosis and did not find changes in plasma cholesterol levels upon BCG treatment in *Apoe*$^{-/-}$ mice and *Ldlr*$^{-/-}$ mice. However, even though *Apoe*$^{-/-}$ and *Ldlr*$^{-/-}$ mice are the most widely used atherosclerosis models, they lack a functional hepatic ApoE-LDLR axis, the predominant route by which cholesterol-enriched lipoprotein remnants are cleared from the circulation (9). Based on our study in *E3L.CETP* mice, with a functional ApoE-LDLR pathway for lipoprotein remnant clearance, we conclude that the cholesterol lowering effect of BCG overrules the effect of immune activation during the development of atherosclerosis, resulting in delayed atherosclerotic plaque formation.

Carotid atherosclerosis is increased in patients with chronic infections and interestingly, the atherosclerosis risk is highest in those with the most prominent inflammatory response, indicating that systemic inflammation contributes to atherosclerosis (43). However, Giral *et al.* (44) compared hypercholesterolemic patients with and without a history of tuberculosis and found that past tuberculosis is not associated with atherosclerosis development. Whether mycobacterial infection has beneficial effects on atherosclerosis in humans related to a reduction in plasma cholesterol remains to be investigated.

In conclusion, our data demonstrate that BCG infection lowers plasma nonHDL-cholesterol levels by accelerating hepatic uptake of cholesterol-enriched lipoprotein remnants and reducing intestinal absorption of dietary cholesterol. Furthermore, BCG delays atherosclerotic plaque formation despite increased immune activation, most likely due to lowering of nonHDL-cholesterol. Because BCG is used as a vaccine for tuberculosis worldwide, the effect of BCG on atherosclerosis in humans is an interesting field of future studies.

ACKNOWLEDGMENTS

We thank Lianne van der Wee-Pals, Trea Streefland, Amanda Pronk, Isabel Mol and Sam van der Tuin (Dept. of Medicine, Div. of Endocrinology, LUMC, Leiden, The Netherlands) as well as Cor Jacobs, Ineke Verschueren, Julia van Tuijl (Dept. of Internal Medicine, Radboud UMC, Nijmegen, The Netherlands) and Anja Kerksiek (Dept. of Clinical Pharmacology, University of Bonn, Germany) for their excellent technical assistance. We thank Reinout van Crevel (Dept. of Internal Medicine, Radboud UMC, Nijmegen, The Netherlands) for outstanding discussions.

FUNDING

This work was supported by a research grant of the Rembrandt Institute of Cardiovascular Science (RICS). Niels P. Riksen was supported by a grant of the Netherlands Heart Foundation (grant 2012T051). Patrick C.N. Rensen is an Established Investigator of the Netherlands Heart Foundation (grant 2009T038).

REFERENCES

1. Libby P, Lichtman AH, Hansson GK: Immune effector mechanisms implicated in atherosclerosis: from mice to humans. Immunity 2013;38:1092-1104
2. Rosenfeld ME, Campbell LA: Pathogens and atherosclerosis: update on the potential contribution of multiple infectious organisms to the pathogenesis of atherosclerosis. Thromb Haemost 2011;106:858-867
3. Westerterp M, Berbee JF, Pires NM, van Mierlo GJ, Kleemann R, Romijn JA, Havekes LM, Rensen PC: Apolipoprotein C-I is crucially involved in lipopolysaccharide-induced atherosclerosis development in apolipoprotein E-knockout mice. Circulation 2007;116:2173-2181
4. Bali P, Tousif S, Das G, van Kaer L: Strategies to improve BCG vaccine efficacy. Immunotherapy 2015;7:945-948
5. Lamb DJ, Eales LJ, Ferns GA: Immunization with bacillus Calmette-Guerin vaccine increases aortic atherosclerosis in the cholesterol-fed rabbit. Atherosclerosis 1999;143:105-113
6. Ovchinnikova OA, Berge N, Kang C, Urien C, Ketelhuth DF, Pottier J, Drouet L, Hansson GK, Marchal G, Back M, Schwartz-Cornil I, Lagranderie M: Mycobacterium bovis BCG killed by extended freeze-drying induces an immunoregulatory profile and protects against atherosclerosis. J Intern Med 2014;275:49-58
7. Westerterp M, van der Hoogt CC, de Haan W, Offerman EH, Dallinga-Thie GM, Jukema JW, Havekes LM, Rensen PC: Cholesteryl ester transfer protein decreases high-density lipoprotein and severely aggravates atherosclerosis in APOE*3-Leiden mice. Arterioscler Thromb Vasc Biol 2006;26:2552-2559
8. de Haan W, van der Hoogt CC, Westerterp M, Hoekstra M, Dallinga-Thie GM, Princen HM, Romijn JA, Jukema JW, Havekes LM, Rensen PC: Atorvastatin increases HDL cholesterol by reducing CETP expression in cholesterol-fed APOE*3-Leiden.CETP mice. Atherosclerosis 2008;197:57-63
9. Berbee JF, Boon MR, Khedoe PP, Bartelt A, Schlein C, Worthmann A, Kooijman S, Hoeke G, Mol IM, John C, Jung C, Vazirpanah N, Brouwers LP, Gordts PL, Esko JD, Hiemstra PS, Havekes LM, Scheja L, Heeren J, Rensen PC: Brown fat activation reduces hypercholesterolaemia and protects from atherosclerosis development. Nat Commun 2015;6:6356
10. Kleinnijenhuis J, Quintin J, Preijers F, Joosten LA, Ifrim DC, Saeed S, Jacobs C, van LJ, de JD, Stunnenberg HG, Xavier RJ, van der Meer JW, van CR, Netea MG: Bacille Calmette-Guerin induces NOD2-dependent nonspecific protection from reinfection via epigenetic reprogramming of monocytes. Proc Natl Acad Sci U S A 2012;109:17537-17542
11. Hirschfeld M, Ma Y, Weis JH, Vogel SN, Weis JJ: Cutting edge: repurification of lipopolysaccharide eliminates signaling through both human and murine toll-like receptor 2. J Immunol 2000;165:618-622
12. Netea MG, Demacker PN, Kullberg BJ, Boerman OC, Verschueren I, Stalenhoef AF, van der Meer JW: Low-density lipoprotein receptor-deficient mice are protected against lethal endotoxemia and severe gram-negative infections. J Clin Invest 1996;97:1366-1372
13. Bligh EG, Dyer WJ: A rapid method of total lipid extraction and purification. Can J Biochem Physiol 1959;37:911-917
14. Rensen PC, van Dijk MC, Havenaar EC, Bijsterbosch MK, Kruijt JK, van Berkel TJ: Selective liver targeting of antivirals by recombinant chylomicrons--a new therapeutic approach to hepatitis B. Nat Med 1995;1:221-225

15. Lutjohann D, Stroick M, Bertsch T, Kuhl S, Lindenthal B, Thelen K, Andersson U, Bjorkhem I, Bergmann KK, Fassbender K: High doses of simvastatin, pravastatin, and cholesterol reduce brain cholesterol synthesis in guinea pigs. Steroids 2004;69:431-438
16. Boon MR, Kooijman S, van Dam AD, Pelgrom LR, Berbee JF, Visseren CA, van Aggele RC, van den Hoek AM, Sips HC, Lombes M, Havekes LM, Tamsma JT, Guigas B, Meijer OC, Jukema JW, Rensen PC: Peripheral cannabinoid 1 receptor blockade activates brown adipose tissue and diminishes dyslipidemia and obesity. FASEB J 2014;28:5361-5375
17. van Tits LJ, Stienstra R, van Lent PL, Netea MG, Joosten LA, Stalenhoef AF: Oxidized LDL enhances pro-inflammatory responses of alternatively activated M2 macrophages: a crucial role for Kruppel-like factor 2. Atherosclerosis 2011;214:345-349
18. Wong MC, van Diepen JA, Hu L, Guigas B, de Boer HC, van Puijvelde GH, Kuiper J, van Zonneveld AJ, Shoelson SE, Voshol PJ, Romijn JA, Havekes LM, Tamsma JT, Rensen PC, Hiemstra PS, Berbee JF: Hepatocyte-specific IKKbeta expression aggravates atherosclerosis development in APOE*3-Leiden mice. Atherosclerosis 2012;220:362-368
19. Katzir Z, Okon E, Ludmirski A, Sherman Y, Haas H: Generalized lymphadenitis following B.C.G. vaccination in an immunocompetent 12-year-old boy. Eur J Pediatr 1984;141:165-167
20. Talbot EA, Perkins MD, Silva SF, Frothingham R: Disseminated bacille Calmette-Guerin disease after vaccination: case report and review. Clin Infect Dis 1997;24:1139-1146
21. Shoaran M, Najafi M, Jalilian R, Rezaei N: Granulomatous hepatitis as a rare complication of Bacillus Calmette-Guerin vaccination. Ann Saudi Med 2013;33:627-629
22. Patel SG, Cohen A, Weiner AB, Steinberg GD: Intravesical therapy for bladder cancer. Expert Opin Pharmacother 2015;16:889-901
23. Gottke MU, Wong P, Muhn C, Jabbari M, Morin S: Hepatitis in disseminated bacillus Calmette-Guerin infection. Can J Gastroenterol 2000;14:333-336
24. Guidi R, Bolli V, Lanza C, Biagetti C, Osimani P, de Benedictis FM: Macronodular hepatosplenic tuberculosis. Acta Radiol Short Rep 2012;1
25. Alghamdi AA, Awan FS, Maniyar IH, Alghamdi NA: Unusual manifestation of extrapulmonary tuberculosis. Case Rep Med 2013;2013:353798
26. Getz GS, Reardon CA: The mutual interplay of lipid metabolism and the cells of the immune system in relation to atherosclerosis. Clin Lipidol 2014;9:657-671
27. Ouellet H, Johnston JB, de Montellano PR: Cholesterol catabolism as a therapeutic target in Mycobacterium tuberculosis. Trends Microbiol 2011;19:530-539
28. Wipperman MF, Sampson NS, Thomas ST: Pathogen roid rage: cholesterol utilization by Mycobacterium tuberculosis. Crit Rev Biochem Mol Biol 2014;49:269-293
29. Pandey AK, Sassetti CM: Mycobacterial persistence requires the utilization of host cholesterol. Proc Natl Acad Sci U S A 2008;105:4376-4380
30. Lovewell RR, Sassetti CM, van der Ven BC: Chewing the fat: lipid metabolism and homeostasis during M. tuberculosis infection. Curr Opin Microbiol 2015;29:30-36
31. Heiniger HJ, Marshall JD: Cholesterol synthesis in polyclonally activated cytotoxic lymphocytes and its requirement for differentiation and proliferation. Proc Natl Acad Sci U S A 1982;79:3823-3827
32. Dabrowski MP, Peel WE, Thomson AE: Plasma membrane cholesterol regulates human lymphocyte cytotoxic function. Eur J Immunol 1980;10:821-827
33. Gatfield J, Pieters J: Essential role for cholesterol in entry of mycobacteria into

macrophages. Science 2000;288:1647-1650

34. Mattos KA, Oliveira VC, Berredo-Pinho M, Amaral JJ, Antunes LC, Melo RC, Acosta CC, Moura DF, Olmo R, Han J, Rosa PS, Almeida PE, Finlay BB, Borchers CH, Sarno EN, Bozza PT, Atella GC, Pessolani MC: Mycobacterium leprae intracellular survival relies on cholesterol accumulation in infected macrophages: a potential target for new drugs for leprosy treatment. Cell Microbiol 2014;16:797-815
35. Kim MJ, Wainwright HC, Locketz M, Bekker LG, Walther GB, Dittrich C, Visser A, Wang W, Hsu FF, Wiehart U, Tsenova L, Kaplan G, Russell DG: Caseation of human tuberculosis granulomas correlates with elevated host lipid metabolism. EMBO Mol Med 2010;2:258-274
36. van der Heide F: Acquired causes of intestinal malabsorption. Best Pract Res Clin Gastroenterol 2016;30:213-224
37. Wouthuyzen-Bakker M, Bodewes FA, Verkade HJ: Persistent fat malabsorption in cystic fibrosis; lessons from patients and mice. J Cyst Fibros 2011;10:150-158
38. Gelzo M, Sica C, Elce A, Dello RA, Iacotucci P, Carnovale V, Raia V, Salvatore D, Corso G, Castaldo G: Reduced absorption and enhanced synthesis of cholesterol in patients with cystic fibrosis: a preliminary study of plasma sterols. Clin Chem Lab Med 2016;54:1461-1466
39. Taylor GO, Bamgboye AE: Serum cholesterol and diseases in Nigerians. Am J Clin Nutr 1979;32:2540-2545
40. Deniz O, Gumus S, Yaman H, Ciftci F, Ors F, Cakir E, Tozkoparan E, Bilgic H, Ekiz K: Serum total cholesterol, HDL-C and LDL-C concentrations significantly correlate with the radiological extent of disease and the degree of smear positivity in patients with pulmonary tuberculosis. Clin Biochem 2007;40:162-166
41. Daniel J, Maamar H, Deb C, Sirakova TD, Kolattukudy PE: Mycobacterium tuberculosis uses host triacylglycerol to accumulate lipid droplets and acquires a dormancy-like phenotype in lipid-loaded macrophages. PLoS Pathog 2011;7:e1002093
42. Weiner J, III, Parida SK, Maertzdorf J, Black GF, Repsilber D, Telaar A, Mohney RP, Arndt-Sullivan C, Ganoza CA, Fae KC, Walzl G, Kaufmann SH: Biomarkers of inflammation, immunosuppression and stress with active disease are revealed by metabolomic profiling of tuberculosis patients. PLoS One 2012;7:e40221
43. Kiechl S, Egger G, Mayr M, Wiedermann CJ, Bonora E, Oberhollenzer F, Muggeo M, Xu Q, Wick G, Poewe W, Willeit J: Chronic infections and the risk of carotid atherosclerosis: prospective results from a large population study. Circulation 2001;103:1064-1070
44. Giral P, Kahn JF, Andre JM, Carreau V, Dourmap C, Bruckert E, Chapman MJ: Carotid atherosclerosis is not related to past tuberculosis in hypercholesterolemic patients. Atherosclerosis 2007;190:150-155

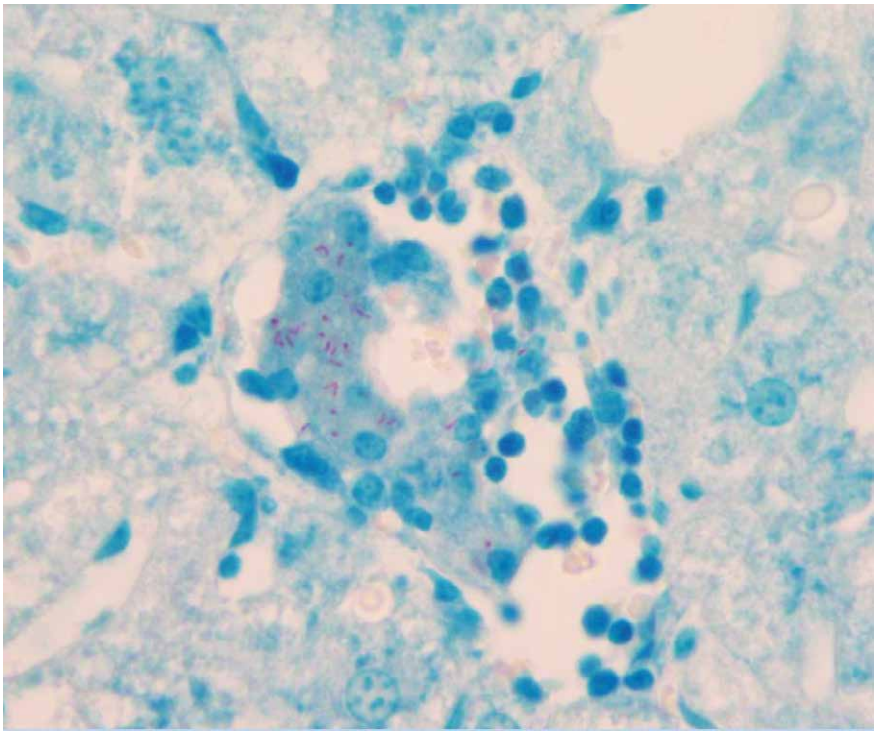

Supplementary figure 1. *E3L.CETP mice fed a WTD were treated with PBS or BCG (0.75 mg; 5x10^6 CFU; i.v.) at baseline (t=0 weeks). Upon sacrifice after 6 weeks, livers were collected and Ziehl-Neelsen (ZN) staining of liver sections was performed. A representative liver section of a BCG-treated mouse is shown.*

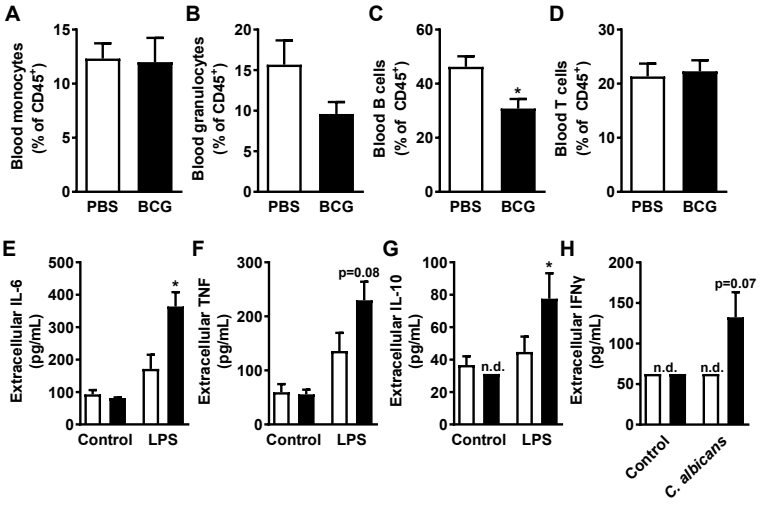

Supplementary figure 2. *E3L.CETP mice fed a WTD were treated with PBS or BCG (0.75 mg; 5x10^6 CFU; i.v.) at baseline (t=0 weeks). After 6 weeks, blood and splenocytes were collected. Within the CD45+ cells in the blood, percentage of monocytes (A), granulocytes (B), B cells (C) and CD3+ T cells (D) was measured. Isolated splenocytes were stimulated with LPS for innate cytokines or C. albicans for adaptive cytokines. Production of IL-6 (E), TNF (F), IL-10 (G) and IFNγ (H) was measured. Values represent means ± SEM (n=6). *p<0.05 vs. PBS.*